Eur. J. Mineral.
2009, **21**, 397–406
Published online November 2008

Ti substitution mechanisms in phlogopites from the Suwalki massif-type anorthosite, NE Poland

OLIVIER NAMUR[1], FRÉDÉRIC HATERT[2,*], FERNANDE GRANDJEAN[3], GARY J. LONG[4], NATACHA KRINS[5], ANDRÉ-MATHIEU FRANSOLET[2], JACQUELINE VANDER AUWERA[1] and BERNARD CHARLIER[1]

[1]Département de Géologie, UR Pétrologie et Géochimie endogènes, B20, Université de Liège, 4000 Liège, Belgium
[2]Département de Géologie, Laboratoire de Minéralogie, B18, Université de Liège, 4000 Liège, Belgium
*Corresponding author, e-mail: fhatert@ulg.ac.be
[3]Département de Physique, B5, Université de Liège, 4000 Liège, Belgium
[4]Department of Chemistry, University of Missouri-Rolla, Missouri 65409-0010, USA
[5]Département de Chimie, Laboratoire de Chimie inorganique structurale (LCIS), B6, Université de Liège, 4000 Liège, Belgium

Abstract: Intercumulus titanian phlogopite occurs in leuco- and gabbro-noritic cumulates from the Suwalki anorthosite massif, NE Poland. The degree of Ti enrichment in the micas ranges from 2.59 to 9.41 wt.% TiO_2. The chemical composition is highly variable for several other elements: Al_2O_3 (13.07–16.75 wt.%), K_2O (7.90–10.16 wt.%), FeO_{tot} (6.92–16.69 wt.%), Fe_2O_3 (0.82–2.95 wt.%), and MgO (9.86–19.54 wt.%), with a Mg/(Fe + Mg) ratio ranging from 0.47 to 0.83. Substitution mechanisms for Ti are proposed, which suggest the presence of exchange vectors involving octahedral and tetrahedral cations. In samples characterized by low Ti contents (0.147–0.239 Ti a.p.f.u.), the Ti incorporation mechanism is: $^{[6]}Ti^{4+} + {}^{[6]}\square = 2(^{[6]}Mg^{2+}, {}^{[6]}Fe^{2+}, {}^{[6]}Mn^{2+})$, where $^{[6]}\square$ corresponds to a vacancy in octahedral coordination (Ti-vacancy). In the two groups with intermediate (0.164–0.326 Ti a.p.f.u.) and high Ti contents (0.477–0.532 Ti a.p.f.u.), the Ti substitution mechanism corresponds to the reaction: $^{[6]}Ti^{4+} + 2(^{[4]}Al^{3+}, {}^{[4]}Fe^{3+}) = (^{[6]}Mg^{2+}, {}^{[6]}Fe^{2+}, {}^{[6]}Mn^{2+}) + 2^{[4]}Si^{4+}$ (Ti-Tschermak). The Mössbauer spectral investigation shows that 0.046–0.167 a.p.f.u. Fe^{3+} occur on the octahedral sites of the structure. The substitution mechanism responsible for the incorporation of Fe^{3+} in phlogopites from Suwalki is $3(^{[6]}Mg^{2+}, {}^{[6]}Fe^{2+}) = 2(^{[6]}Al^{3+}, {}^{[6]}Fe^{3+}) + {}^{[6]}(M^{3+}\text{-vacancy})$. The use of the Ti content of phlogopite as geothermometer reveals crystallization temperatures from 729 ± 15 to 874 ± 15 °C for the phlogopites.

Key-words: phlogopite, titanium, substitution mechanisms, Mössbauer spectroscopy, geothermometry.

Introduction

Occurring in many plutonic rocks over a wide range of bulk compositions and from different tectonic environments (Feldstein *et al.*, 1996), the common mineral phlogopite, $KMg_3[(Si_3Al)O_{10}](OH)_2$, shows numerous substitutions on its different crystallographic sites. Among the cationic substitutions, those involving Ti and Al have been largely investigated (*e.g.* Arima & Edgar, 1981; Dymek, 1983; Abrecht & Hewitt, 1988; Waters & Charnley, 2002; Cesare *et al.*, 2003; Scordari *et al.*, 2006; Matarrese *et al.*, 2008). While the dominant mechanism for the Al substitution is represented by the Tschermak's reaction, *i.e.* $^{[6]}R^{2+} + {}^{[4]}Si^{4+} = {}^{[6]}Al^{3+} + {}^{[4]}Al^{3+}$, many models for the Ti substitution have been proposed by various authors. Except Kunitz (1936), all of them consider Ti in octahedral coordination and, according to Dymek (1983), Ti^{4+} substitutes thus for octahedral cations only or is inserted by mechanisms involving both octahedral and tetrahedral cations (Dymek, 1983).

The most important mechanisms by which Ti enters into the phlogopite structure are represented by the following reactions: (1) $R^{2+} + 2Si^{4+} = Ti^{4+} + 2Al^{3+}$, where R^{2+} is an unspecified divalent cation (Robert, 1976); (2) $2R^{2+} = Ti^{4+} + \square$ (Forbes & Flower, 1974; Matarrese *et al.*, 2008); and (3) $R^{2+} + 2OH^{-} = Ti^{4+} + 2O^{2-}$ (Dyar *et al.*, 1993; Scordari *et al.*, 2006; Cesare *et al.*, 2008; Matarrese *et al.*, 2008). Dymek (1983) has proposed that a combination of several Ti-substitution mechanisms is generally required for the explanation of all the Ti content variations observed in natural phlogopites. By synthetizing Ti-bearing phlogopites along the compositional joins corresponding to these reactions, the first two mechanisms have been experimentally corroborated (Forbes & Flower, 1974; Robert, 1976; Abrecht & Hewitt, 1988).

The deprotonation substitution mechanism, $R^{2+} + 2OH^{-} = Ti^{4+} + 2O^{2-}$, (Dyar *et al.*, 1993) has been neglected in investigations using electron microprobe because of the lack of Fe^{2+}/Fe^{3+} ratio and H_2O content determinations. However, crystal structure analyses (Cruciani & Zanazzi, 1994; Scordari *et al.*, 2006; Matarrese *et al.*, 2008), Mössbauer spectral studies (Scordari *et al.*, 2006; Matarrese *et al.*, 2008) and ion probe microanalyses

0935-1221/09/0021-1894 $ 4.50
DOI: 10.1127/0935-1221/2009/0021-1894

(Virgo & Popp, 2000; Righter *et al.*, 2002; Matarrese *et al.*, 2008) have revealed that deprotonation can play a major role in magmatic phlogopites.

As a result of a great number of experimental studies, it is clearly established that the Ti incorporation increases with temperature and decreases with pressure (Forbes & Flower, 1974; Robert, 1976; Edgar *et al.*, 1976; Arima & Edgar, 1981; Tronnes *et al.,* 1985). As examples, Ti-rich phlogopite is a major mineral in lamproites and other potassic rocks (Mitchell, 1985; Wagner & Velde, 1986; Mitchell & Bergman, 1991), Guidotti *et al.* (1977) and Patiño Douce *et al.* (1993) have showed that magmatic phlogopite may contain up to 6 wt.% TiO_2, at high temperature, near the melting conditions. However, the more Ti-rich phlogopites were discovered in alkali-rich rocks. As an example, Ibhi *et al.* (2005) have reported phlogopites with up to 13.85 wt.% TiO_2 occurring in inclusions in calcite carbonatite from Jbel Saghro, Anti-Atlas, Morocco.

The occurrence of Ti-rich phlogopites with TiO_2 contents between 2.59 and 9.41 wt.%, in cumulates of the Suwalki anorthosite massif, was the starting point of this study. Results of electron-microprobe and Mössbauer spectral analyses on these samples reveal an important Ti and, to a lesser extent, Al enrichment, and are thus used to discuss the substitution mechanisms of Ti^{4+}.

Geological setting and petrography

Located in the north-eastern part of Poland, the Mazury complex is a large body (200 × 40 km) of Mesoproterozoic age – about 1.5 Ga according to Morgan *et al.* (2000) and Dörr *et al.* (2002). It is dominated by granitoid rocks, but also by noritic and anorthositic plutons (Dörr *et al.*, 2002). The Mazury complex interestingly includes three anorthosite massifs: Ketrzyn, Sejny, and Suwalki. These anorthosites together with (Rapakivi-) granites of the Mazury complex constitute a typical AMCG (Anorthosite–Mangerite–Charnockite–(Rapakivi-) Granite) suite.

The Suwalki massif-type anorthosite is an elliptic igneous body of about 250 km^2 intruded in the eastern part of the Mazury complex. As the Suwalki massif is buried under a 580–1200 m thick Phanerozoic cover, it has been essentially explored by drilling. It has a dome shape with 140 km^2 of anorthosite in central part and is surrounded by gabbronorites and diorites. Several Fe–Ti ore deposits have been recognized and ore reserves have been estimated at about 1250 Gt.

The analytical work reported herein was performed on intercumulus phlogopites from typical (gabbro-) noritic cumulates of the Suwalki anorthosite massif. These phlogopite-bearing rocks come from drill cores of four localities: Udryn (U); Jeleniewo (J); Krzemianka (K); and Lopuchowo (Pig). Two cumulus assemblages may be distinguished. First, the norite is composed by plagioclase, orthopyroxene, magnetite, and ilmenite. The second type of rocks, the gabbronorite, contains the same minerals with additional phases, clinopyroxene and apatite and to a lesser extent, quartz, and potassium feldspar. The two types of cumulates are related to the same differentiation trend of the parental liquid and correspond to different evolution stages. Their phlogopite content ranges from about 1 to 15 vol.%. All the samples contain a Ti-saturating phase, which is always ilmenite. Magnetite and plagioclase, representing respectively the Fe- and Al-saturating phases, are present in all the selected samples. In the more evolved gabbronoritic samples (K57-02 and Pig-05), quartz and potassium feldspar are relatively abundant (> 5 vol.%).

Analytical methods

The composition of phlogopites for major elements was obtained with a CAMECA SX50 electron-microprobe at the Geology Institute of the Ruhr-Universität Bochum (Germany). Standard operating conditions were excitation voltage of 15 kV, beam current of 10 nA and peak-count of 30 s. The following standards were used for $K\alpha$ X-ray lines: synthetic pyrope for Si, Mg, and Al; synthetic andradite for Fe and Ca; synthetic spessartine for Mn; synthetic rutile for Ti; jadeite for Na; synthetic Ba- and K-glasses for Ba and K; synthetic NaCl for Cl; topaz for F. Overlapping of the $K\alpha_1$ X-ray lines of Ba and Ti was tested using benitoite and found negligible. Crystals used for the electron-microprobe analysis were: TAP for Mg, Si, and Al; PET for Ti, Ba, K, Ca, and Na; LIF for Ni, Mn, and Fe; PC_2 for F and Cl. Raw data were corrected with the CATZAF software. This study has been realized on 24 samples, with a total of 110 punctual analyses. Average results are given in Table 1.

X-ray powder diffraction measurements were performed with a Panalytical PW-3710 diffractometer (Fe$K\alpha$ radiation, λ = 1.9373 Å), in order to check the purity of the samples before their investigation by Mössbauer spectroscopy. Several crystals of phlogopite from samples U4-03, PIG-06, and K20-05 were also investigated by X-ray single-crystal diffraction. These crystals were measured on a Bruker P4 four-circle diffractometer (University Liège, Mo$K\alpha$ radiation, λ = 0.71073 Å) and on an Oxford Diffraction Gemini A Ultra 4-circle diffractometer (Mo$K\alpha$ radiation).

The iron-57 Mössbauer spectra have been measured at 85 or 90 K on a constant acceleration spectrometer which utilized a rhodium matrix cobalt-57 source and was calibrated at room temperature with α-iron foil. The absorbers contained typically 5–10 mg/cm^2 of mineral mixed with boron nitride. The spectra have been fit with four Lorentzian doublets and assigned as discussed below. The estimated uncertainties in the Mössbauer spectral parameters are *ca.* ±0.005 mm/s for the isomer shifts, ±0.01 mm/s for the quadrupole splitting and the linewidth, and ±0.5 % for the relative areas. The uncertainty on the Fe^{2+} percentage and on the Fe^{2+}/Fe^{3+} ratio has been obtained from different fits carried out from different initial parameters and represents the statistical error in the fits.

Eighteen phlogopite samples were investigated by infrared spectroscopy. Phlogopite samples were separated from rock powders (60–150 μm) using dense liquid and a Frantz isodynamic separator. The final purification was realized by collecting the phlogopite flakes on a piece of abrasive paper

Table 1. Electron-microprobe analyses of phlogopites from Suwalki.

Samples	Pig-01	Pig-02	Pig-04	Pig-05	Pig-06	K2-01	K2-02	K2-05	K12-05	K20-03	K20-04	K20-05	K22-01	K57-02	U2-01	U2-03	U4-01	U4-02	U4-03	U5-02	J1-02	J2-01	J2-02	J2-03
n^*	4	6	4	3	4	4	4	3	3	8	7	4	6	5	2	4	5	5	5	5	5	6	4	4
SiO_2	37.02	36.25	36.66	37.20	36.55	35.45	35.17	36.12	36.51	36.55	36.42	36.09	36.67	35.57	37.19	37.79	37.22	37.40	36.33	37.19	37.05	37.33	37.05	35.80
TiO_2	4.34	4.90	4.80	4.23	4.27	3.66	2.89	3.57	5.54	5.18	9.39	8.44	9.41	2.59	5.32	4.26	4.32	4.30	5.75	5.25	4.45	3.34	5.21	4.41
Al_2O_3	13.28	13.41	13.99	15.35	14.25	15.10	15.49	14.69	14.56	14.60	13.27	14.04	13.19	16.75	14.08	13.07	13.58	13.35	14.73	13.94	13.83	13.68	13.97	14.65
FeO^{**}	15.70	12.97	12.42	19.69	9.86	8.31	8.09	7.04	11.00	8.76	10.84	8.36	11.50	6.92	10.65	10.67	10.73	10.67	9.80	8.68	11.43	8.68	9.14	7.98
$Fe_2O_3^{**}$		2.95	1.71		1.78					1.72		2.04							0.82	1.70				
MgO	14.25	14.84	15.08	9.86	16.76	19.00	19.29	19.54	16.21	17.27	14.59	15.60	14.18	18.89	16.81	17.30	17.12	17.00	16.94	17.39	16.54	18.85	17.54	19.06
MnO	0.11	0.26	0.14	0.39	0.07	0.03	0.05	0.04	0.04	0.05	0.04	0.01	0.04	0.02	0.01	0.09	0.05	0.06	0.02	0.02	0.04	0.03	0.03	0.03
BaO	0.52	0.55	0.42	0.62	1.11	0.58	0.65	0.49	0.45	0.76	0.44	0.81	0.25	0.49	1.18	0.44	0.84	0.56	0.79	0.98	0.45	0.85	0.19	0.57
CaO	0.01	0.02	0.02	0.01	0.03	0.01	0.04	0.03	0.04	0.00	0.01	0.02	0.01	0.01	0.07	0.01	0.01	0.03	0.02	0.01	0.18	0.03	0.02	0.02
Na_2O	0.12	0.09	0.04	0.04	0.06	0.57	0.76	1.08	0.11	0.30	0.09	0.12	0.10	0.47	0.08	0.05	0.08	0.08	0.48	0.11	0.05	0.15	0.08	0.48
K_2O	9.75	9.57	10.06	9.53	9.57	9.02	8.38	7.90	9.95	9.84	9.83	9.99	10.00	9.60	9.76	9.84	9.72	9.71	9.53	9.94	9.62	9.13	10.16	9.54
F	1.37	0.65	1.05	0.43	0.41	0.99	1.04	0.84	0.26	0.35	0.39	0.95	0.49	0.06	0.89	1.54	1.46	0.60	0.28	0.89	0.35	0.81	0.56	0.82
Cl	0.09	0.09	0.00	0.11	0.00	0.03	0.03	0.03	0.00	0.00	0.04	0.00	0.05	0.02	0.00	0.04	0.03	0.03	0.00	0.04	0.02	0.02	0.02	0.02
$H_2O_{calc.}$	3.28	3.63	3.49	3.74	3.78	3.47	3.42	3.54	3.89	3.87	3.83	3.59	3.79	3.93	3.61	3.25	3.28	3.68	3.91	3.61	3.81	3.58	3.74	3.59
$H_2O_{meas.}$		2.10	1.93		1.95					0.70		2.97							1.05	0.80				
Total***	99.81	100.19	99.88	101.21	98.48	96.23	95.31	94.91	98.55	99.25	99.19	100.05	99.68	95.33	99.64	98.33	98.45	97.46	99.40	99.73	97.81	96.47	97.68	96.95
Cation numbers on the basis of 22 charges per formula unit																								
$^{[4]}Si$	2.784	2.726	2.763	2.798	2.755	2.666	2.651	2.723	2.746	2.748	2.739	2.714	2.758	2.675	2.797	2.849	2.799	2.820	2.739	2.804	2.793	2.814	2.793	2.698
$^{[4]}Al$	1.177	1.189	1.237	1.202	1.245	1.334	1.349	1.277	1.254	1.252	1.176	1.244	1.169	1.325	1.203	1.151	1.201	1.180	1.261	1.196	1.207	1.186	1.207	1.302
Sum	3.961	3.915	4.000	4.000	4.000	4.000	4.000	4.000	4.000	4.000	3.915	3.958	3.926	4.000	4.000	4.000	4.000	4.000	4.000	4.000	4.000	4.000	4.000	4.000
$^{[6]}Ti$	0.246	0.277	0.272	0.239	0.242	0.207	0.164	0.202	0.313	0.293	0.531	0.477	0.532	0.147	0.301	0.241	0.244	0.244	0.326	0.297	0.252	0.190	0.295	0.250
$^{[6]}Al$	–	–	0.006	0.158	0.021	0.005	0.027	0.028	0.036	0.043	–	–	–	0.160	0.044	0.010	0.003	0.006	0.048	0.042	0.021	0.029	0.034	0.000
$^{[6]}Fe$	0.987	0.983	0.879	1.238	0.722	0.523	0.510	0.444	0.692	0.648	0.682	0.641	0.724	0.435	0.670	0.673	0.675	0.673	0.664	0.644	0.720	0.55	0.576	0.503
$^{[6]}Mg$	1.597	1.664	1.695	1.106	1.883	2.130	2.168	2.196	1.817	1.936	1.636	1.749	1.589	2.117	1.884	1.944	1.919	1.910	1.903	1.953	1.858	2.118	1.970	2.142
$^{[6]}Mn$	0.007	0.017	0.009	0.025	0.005	0.002	0.003	0.003	0.002	0.003	0.002	0.000	0.003	0.001	0.001	0.006	0.003	0.004	0.001	0.001	0.002	0.002	0.002	0.002
Sum	2.836	2.940	2.861	2.766	2.872	2.866	2.873	2.872	2.860	2.922	2.851	2.868	2.848	2.860	2.900	2.874	2.845	2.836	2.943	2.937	2.855	2.885	2.877	2.896
Vacancies	0.164	0.060	0.139	0.234	0.128	0.134	0.127	0.128	0.140	0.078	0.149	0.132	0.152	0.140	0.100	0.126	0.155	0.164	0.057	0.063	0.068	0.115	0.123	0.104
$^{[12]}Ba$	0.015	0.016	0.012	0.018	0.033	0.017	0.019	0.014	0.013	0.022	0.013	0.024	0.007	0.015	0.035	0.013	0.025	0.016	0.023	0.029	0.013	0.025	0.006	0.017
$^{[12]}Ca$	0.001	0.002	0.001	0.001	0.002	0.000	0.003	0.002	0.003	0.000	0.001	0.001	0.001	0.001	0.005	0.000	0.001	0.002	0.001	0.001	0.015	0.003	0.002	0.002
$^{[12]}Na$	0.017	0.013	0.006	0.006	0.008	0.083	0.111	0.158	0.016	0.043	0.013	0.017	0.014	0.069	0.012	0.007	0.011	0.012	0.070	0.016	0.007	0.021	0.011	0.070
$^{[12]}K$	0.935	0.918	0.967	0.914	0.920	0.866	0.806	0.759	0.954	0.944	0.943	0.959	0.959	0.921	0.936	0.946	0.933	0.934	0.916	0.956	0.925	0.878	0.977	0.917
Sum	0.968	0.949	0.987	0.939	0.963	0.967	0.939	0.935	0.987	1.010	0.970	1.001	0.981	1.005	0.988	0.966	0.969	0.964	1.011	1.002	0.960	0.927	0.995	1.006
Vacancies	0.032	0.051	0.013	0.061	0.037	0.033	0.061	0.065	0.013	−0.010	0.030	−0.001	0.019	−0.005	0.012	0.034	0.031	0.036	−0.011	−0.002	0.040	0.073	0.005	−0.006
F	0.326	0.156	0.250	0.103	0.098	0.236	0.248	0.200	0.060	0.084	0.093	0.225	0.116	0.015	0.212	0.366	0.347	0.143	0.064	0.211	0.082	0.193	0.133	0.194
Cl	0.011	0.012	–	0.014	–	0.004	0.004	0.004	–	–	0.004	–	0.006	0.002	–	0.005	0.004	0.004	0.003	0.006	0.003	0.003	0.002	0.002
OH (calc.)****	1.663	1.833	1.750	1.883	1.902	1.760	1.749	1.796	1.940	1.916	1.903	1.775	1.878	1.983	1.788	1.629	1.650	1.853	1.933	1.783	1.915	1.804	1.866	1.804
XMg*****	0.62	0.63	0.66	0.47	0.72	0.80	0.81	0.83	0.72	0.75	0.71	0.73	0.69	0.83	0.74	0.74	0.74	0.74	0.74	0.75	0.72	0.79	0.77	0.81
T (°C)******	764	784	785	729	789	799	775	808	818	819	874	867	868	770	818	795	796	796	828	821	794	786	828	822

Analyst: H.J. Bernhardt. * n = number of ponctual analyses. ** Values calculated from the Fe^{2+}/Fe^{3+} ratio obtained by Mössbauer spectroscopy. *** Totals were calculated with the $H_2O_{calc.}$ values. **** Obtained by the relation OH = 2 − (F + Cl). ***** XMg = Mg/(Mg + Fe). ****** Temperatures obtained with the equation of Henry *et al.* (2005).

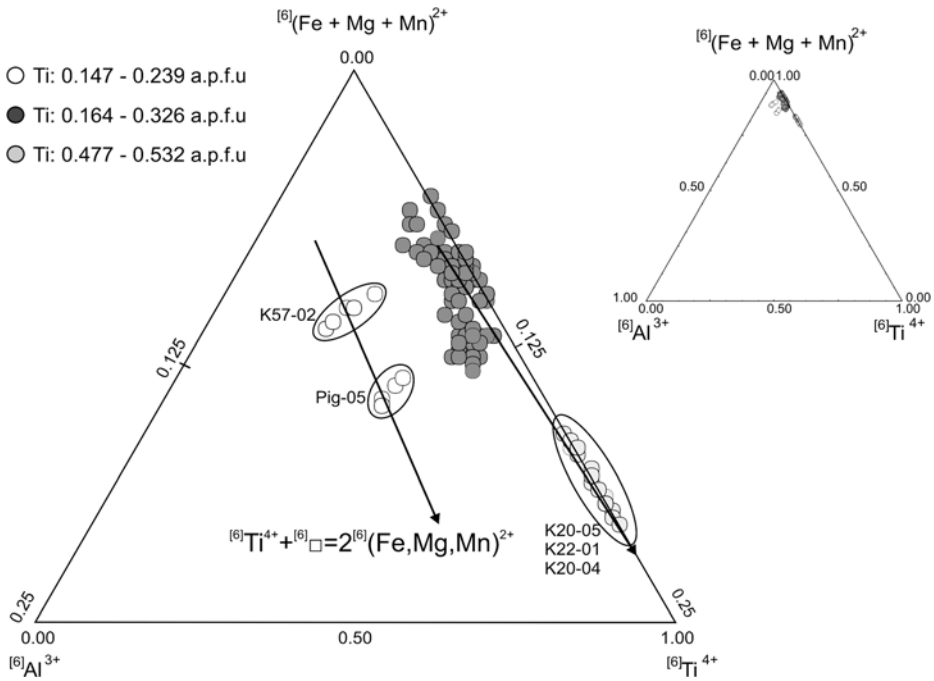

Fig. 1. Ternary diagram ($^{[6]}Mg^{2+}$ + $^{[6]}Fe^{2+}$ + $^{[6]}Mn^{2+}$) – $^{[6]}Ti^{4+}$ – $^{[6]}Al^{3+}$. The arrows symbolize the Ti substitution mechanisms.

and by hand-picking beneath the binocular lens. The purity of the concentrates was estimated as > 99 % by optical microscopy.

The infrared spectra were recorded with a Nicolet NEXUS spectrometer, from 50 scans with a 2 cm^{-1} resolution, over 400–4000 cm^{-1} region. The samples were prepared by intimately mixing 2 mg (±0.1) of sample with KBr in order to obtain a 150 mg homogeneous pellet which was subsequently dried for a few hours at 120 °C. To prevent water contamination, the measurements were performed under a dry air purge.

Thermogravimetric analysis and differential scanning calorimetric analyses were carried out simultaneously using a STA449C NETZSCH thermal analyser. Measurements were performed in a platinum crucible under N_2 atmosphere in a temperature range from 25 to 1400 °C with a heating rate of 600 °C/h.

Results

Phlogopites composition and structural formulae

Various normalization procedures known from the literature are proposed for the interpretation of phlogopite chemical analyses. The normalization model on a basis of 22 charges has been chosen, because this normalization has for great advantage to maintain charge balance. Calculations following this method imply that vacancies are mainly located on both the octahdral sites and the 12-fold-coordinated site (Rancourt *et al.*, 2001). The main disadvantage of this calculation model is that results are directly affected by valence state of iron and variations in the H_2O content. Two alternative calculation methods, following the relations *All cations* – (*Na* + *K* + *Ca* + *Ba*) = 7 (Ludington & Munoz, 1975; Dymek, 1983; Cruciani & Zanazzi, 1994; Feldstein *et al.*, 1996; Waters & Charnley, 2002), and (*Na* + *K* + *Ca* + *Ba*) = 1, are not appropriate because vacancies are common on the octahedral and interlayer sites of the phlogopite structure (Rieder *et al.*, 1998). Nevertheless, preliminary calculations according to these two last models were also performed, and led to similar conclusions than those obtained with a basis of 22 charges.

The chemical composition of the Ti-rich phlogopites from Suwalki is rather variable. SiO_2, in tetrahedral coordination, ranges from 35.17 to 37.79 wt.%, whereas Al_2O_3, partially in both tetrahedral and octahedral sites, varies from 13.07 to 16.75 wt.%. Octahedral elements also display a range of concentration: TiO_2 (2.59–9.41 wt.%), FeO_{tot} (6.92–19.69 wt.%), Fe_2O_3 (0.82–2.95 wt.%), and MgO (9.89–19.54 wt.%). The K_2O-content varies from 7.90 to 10.16 wt.%; Na_2O and CaO are below 1.1 and 0.2 wt.%, respectively, and are not correlated with BaO (0.25–1.18 wt.%). The phlogopites of Suwalki contain less than 0.10 wt.% of Cl, and a moderate amount of F (0.06–1.54 wt.%). All the analysed grains are homogeneous and no zoning patterns have been detected.

In the ternary diagram $^{[6]}Ti^{4+}$ – $^{[6]}Al^{3+}$ – ($^{[6]}Mg^{2+}$ + $^{[6]}Fe^{2+}$ + $^{[6]}Mn^{2+}$) (Fig. 1), phlogopite samples are splitted into three groups. The first group is characterized by an intermediate content of $^{[6]}Ti^{4+}$ and $^{[6]}Al^{3+}$ (0.164–0.326 $^{[6]}Ti^{4+}$ a.p.f.u.; 0.000–0.048 $^{[6]}Al^{3+}$ a.p.f.u.). The two samples (K57-02 and Pig-05) belonging to the second group are relatively poor in $^{[6]}Ti^{4+}$ (0.147–0.239 a.p.f.u.) but highly enriched in $^{[6]}Al^{3+}$ (0.158–0.160 a.p.f.u.). Finally, the third group (samples K20-04, K20-05, and K22-01) shows an important $^{[6]}Ti^{4+}$ content (0.477–0.532 a.p.f.u.) and is completely $^{[6]}Al^{3+}$-free.

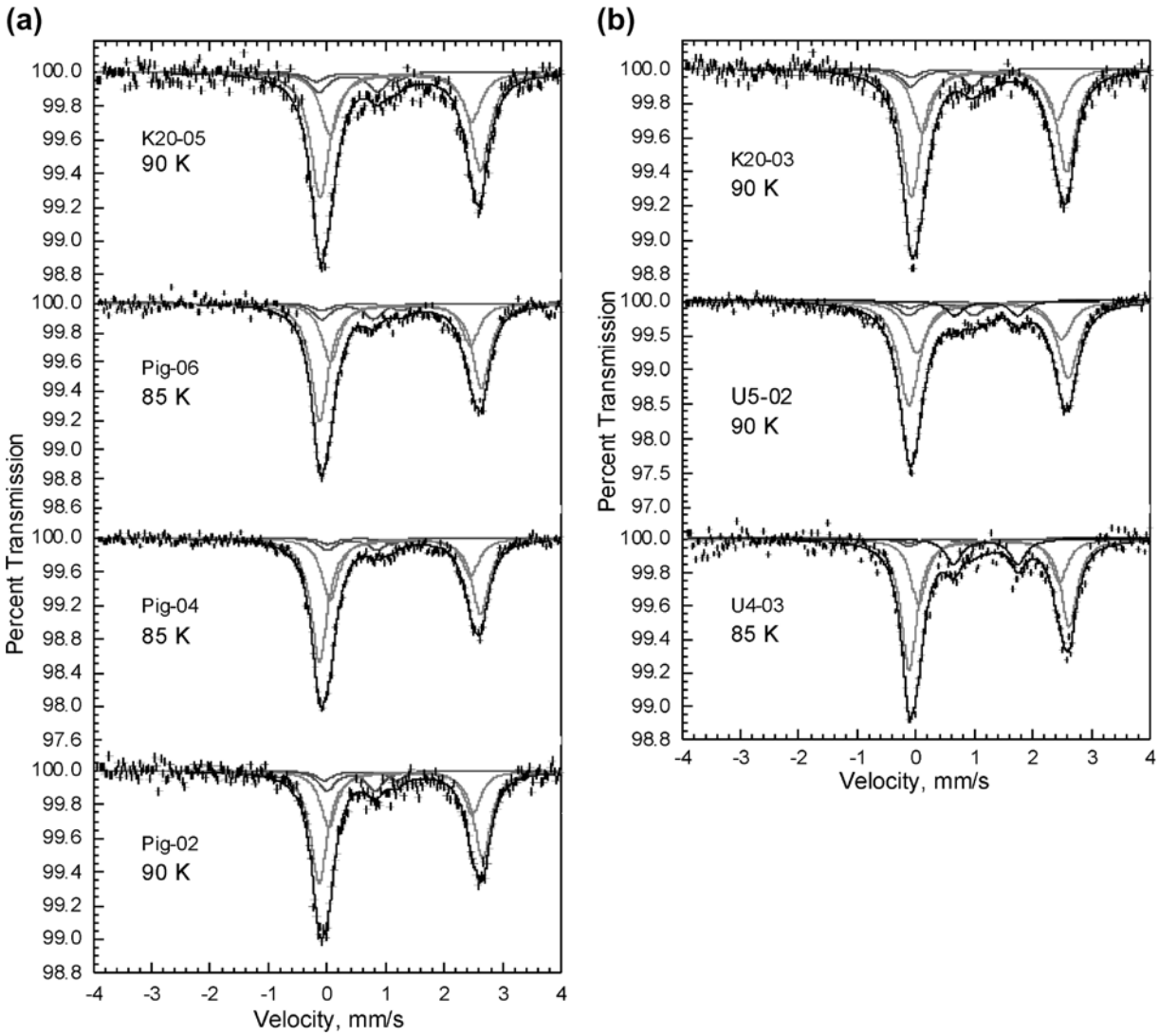

Fig. 2. The Mössbauer spectra of phlogopites from Suwalki. (a): Samples K20-05, Pig-06, Pig-04, and Pig-02. (b): Samples K20-03, U5-02, and U4-03.

X-ray diffraction results

The X-ray powder diffraction patterns of the samples used for the Mössbauer spectral study showed that samples PIG-02 and K20-05 are constituted by pure phlogopite. Minor amounts of ilmenite (PIG-06, U4-03), plagioclase (PIG-04), apatite-(CaF) (PIG-04), and augite (U4-03, U5-02) were also detected in some samples.

Due to the poor crystallinity of the samples, it was impossible to obtain the orientation matrix and unit-cell parameters from the single-crystals investigated with the P4 diffractometer equipped with a point detector. The Gemini A Ultra diffractometer equipped with a CCD detector allowed to measure two crystals of sample K20-05 at 100 K. Both crystals were poorly crystalline, and exhibited a strong powder-like behaviour; however, one of the crystals (size 240 × 170 × 50 μm) showed more distinct diffraction spots overprinted on the powder pattern. Three hundred frames with a spatial resolution of 1° were collected by the φ/ω scan technique, with a counting time of 25 s per frame, in the range $-6 \leq h \leq 7$, $-12 \leq k \leq 9$, $-13 \leq l \leq 12$. A total of 1571 reflections were extracted from these frames, corresponding to 541 unique reflections. The unit-cell parameters refined from these reflections are a = 5.378(4), b = 9.309(9), c = 10.20(1) Å, and β = 100.11(7)°. Data were corrected for Lorenz polarisation and absorption effects, the latter with a numerical method included in the CrysAlisRED package (Oxford Diffraction, 2002). Unfortunately, all attempts to refine the crystal structure from these data failed, probably due to the poor crystallinity of the sample (R_1 above 12 %).

Mössbauer spectroscopy

The Mössbauer spectra of seven samples are shown in Fig. 2. The presence of a major quadrupole doublet with an isomer shift of *ca.* 1.2 mm/s confirms that the majority of the iron ions

Table 2. The Mössbauer spectral hyperfine parameters of phlogopites from Suwalki.

Parameter	Sample	T, K	Fe^{2+}, *M*1	Fe^{2+}, *M*2	Fe^{3+}, *M*1	Fe^{3+}, *M*2
δ,[a] mm/s	K20-05	90	1.270	1.250	0.502	0.366
	Pig-06	85	1.255	1.257	0.578	0.350
	Pig-04	85	1.251	1.245	0.563	0.429
	Pig-02	90	1.255	1.260	0.571	0.407
	K20-03	90	1.250	1.260	0.582	0.439
	U5-02	90	1.254	1.243	0.582	0.432
	U4-03	85	1.252	1.253	0.555	0.424
ΔE_Q, mm/s	K20-05	90	2.40	2.74	1.32	0.99
	Pig-06	85	2.39	2.76	1.35	0.88
	Pig-04	85	2.40	2.76	1.10	0.85
	Pig-02	90	2.45	2.80	1.23	0.82
	K20-03	90	2.28	2.65	1.30	1.08
	U5-02	90	2.47	2.72	1.38	1.12
	U4-03	85	2.41	2.74	1.33	1.09
Γ, mm/s	K20-05	90	0.38	0.38	0.38	0.38
	Pig-06	85	0.36	0.36	0.36	0.36
	Pig-04	85	0.35	0.35	0.35	0.35
	Pig-02	90	0.34	0.34	0.34	0.34
	K20-03	90	0.38	0.38	0.38	0.38
	U5-02	90	0.42	0.42	0.42	0.42
	U4-03	85	0.33	0.33	0.33	0.33
Area, %	K20-05	90	27.1	54.2	6.2	12.5
	Pig-06	85	28.8	57.6	4.6	9.2
	Pig-04	85	29.7	59.3	3.7	7.3
	Pig-02	90	27.9	55.8	5.5	11.0
	K20-03	90	27.4	54.8	5.9	11.8
	U5-02	90	28.8	57.6	4.5	9.1
	U4-03	85	31.1	62.2	2.2	4.5

[a]Relative to room temperature a-iron foil. The relative areas of the *M*1 and *M*2 sites have been constrained to be in a ratio of one to two.

are present as Fe^{2+}. The asymmetry in this doublet results from texture, a texture that is usually observed in these types of layered minerals. Because the Fe^{2+} and Fe^{3+} ions occupy the octahedral *M*1 and *M*2 sites in phlogopite, each of their contributions to the Mössbauer spectra has been fitted with two asymmetric doublets, whose relative areas have been constrained to 1:2, in agreement with the relative populations of the *M*1 and *M*2 sites. The Mössbauer spectra of U5-02 and U4-03 exhibit a fifth doublet whose hyperfine parameters are compatible with the presence of augite previously observed by X-ray powder diffraction. The resulting spectral hyperfine parameters are given in Table 2.

The assignment of the four doublets is in agreement with the literature (Coey, 1984; Badreddine *et al.*, 2000). The Fe^{3+} doublets have isomer shift and quadrupole splitting values, which correspond to octahedral Fe^{3+} in the *M*1 and *M*2 sites (Coey, 1984). The quadrupole splitting at the Fe^{3+} *M*1 sites is larger than that at the Fe^{3+} *M*2 sites, whereas the quadrupole splitting at the Fe^{2+} *M*1 sites is smaller than that at the Fe^{2+} *M*2 sites. This difference occurs because the valence and lattice contributions to the electric field gradient at the Fe^{2+} sites have opposite signs (Dyar, 1987). Hence, the lattice contribution at the *M*1 site is larger than at the *M*2 site. For the Fe^{3+} ions, the only contribution to the electric field gradient is the lattice contribution and, hence, the quadrupole splitting at the Fe^{3+} *M*1 sites is larger than that at the Fe^{3+} *M*2 sites.

Table 3. The Mössbauer spectral derived parameters[a] for the phlogopite samples from Suwalki.

Sample	T, K	% Fe^{2+}	Fe^{2+}/Fe^{3+}
K20-05	90	82(1)	4.9(4)
Pig-06	85	86(1)	6.3(3)
Pig-04	85	89(1)	8.1(3)
Pig-02	90	83(2)	5.1(5)
K20-03	90	85(2)	5.9(4)
U5-02	90	85(2)	5.8(4)
U4-03	85	93(3)	14.0(6)

[a]Based on the phlogopite octahedral *M*1 and *M*2 site iron(II) and iron(III) occupancies.

The percentages of Fe^{2+} and the Fe^{2+}/Fe^{3+} ratio, deduced from the relative areas of the four doublets, are given in Table 3, and were used to calculate the Fe_2O_3 contents reported in Table 1. Because the Mössbauer spectra were obtained at 85 or 90 K, the Fe^{2+} and Fe^{3+} recoil free fractions may be assumed to be equal and the uncertainty on the Fe^{2+} percentage is reduced as compared to any values obtained from a spectrum obtained at 295 K.

K20-05 with the highest Ti substitution shows the smallest Fe^{2+}/Fe^{3+} ratio. U4-03 shows the largest Fe^{2+}/Fe^{3+} ratio. There is no obvious correlation between the Fe^{2+}/Fe^{3+} ratio and the amount of TiO_2 or Al_2O_3.

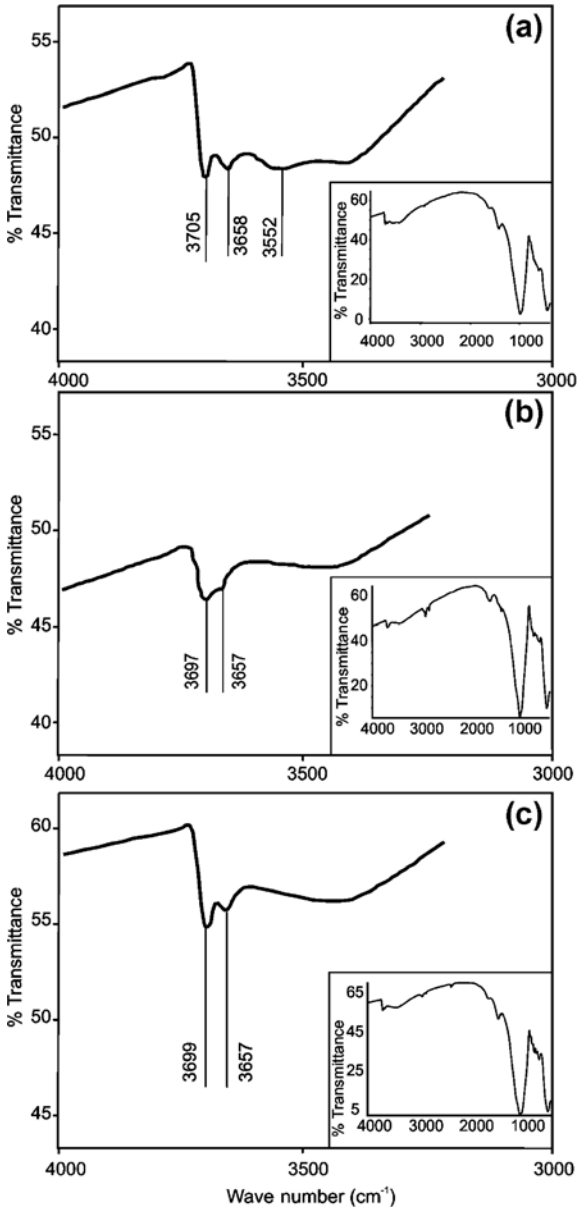

Fig. 3. Selected infrared spectra of phlogopites from Suwalki, in the OH^- stretching region (3200–4000 cm^{-1}). Insets show the complete spectra in the 400–4000 cm^{-1} wave number range. Numbers shown in vertical position correspond to wave number of the peaks. (a): Sample K57-02, (b): Sample Pig-04, and (c): Sample U5-02.

Infrared spectroscopy and thermal analysis

The 18 infrared spectra are similar, with a small variation in the intensity and the position of several absorption bands. Selected spectra are shown on Fig. 3 and present 2 main massifs. The first one is located around 1000 cm^{-1}, and corresponds to vibrations of the SiO_4 tetrahedron, whereas the other is located roughly at 500 cm^{-1}, and corresponds to lattice vibrations.

Other absorption bands, due to the vibrations of OH^- groups, fall between 3400 and 3800 cm^{-1} (Petit *et al.*, 1995). In this range, 2 to 3 peaks can be recognized. The first one is located between 3695 and 3705 cm^{-1} (Fig. 3a–c) and results from the vibrations of OH groups interacting with 3 Mg atoms, thus suggesting a magnesian environment (Mg_3OH). Another peak with a very low intensity is centred on 3657 cm^{-1}. Wilkins (1967) and Vedder & Wilkins (1969) have attributed this band to the vibrations of $Mg_2R^{3+}OH$ and Papin *et al.* (1997) further consider that it corresponds to Mg_2AlOH. Finally, some spectra show a last band around 3552 cm^{-1} (Fig. 3a). The attribution of this peak is still debated, since Farmer (1971) considers this band to be related to the $Fe^{2+}Fe^{3+}OH$ group, whereas Robert *et al.* (1993, 1995) assign this peak to Mg_2OH. In conclusion, this last band is a good indicator of a weak dioctahedral component present in some samples.

Thermal analyses were performed in order to obtain a direct determination of the water content of phlogopites. However, the thermal curves were of poor quality, with a progressive weight loss between *ca.* 200 and 1000 °C. The major weight loss, occurring around *ca.* 1150 °C, probably corresponds to the loss of OH groups by the phlogopite structure, and served us to obtain the H_2O contents reported in Table 1.

Discussion

Ti substitution mechanisms

The Ti substitution affects the three groups of phlogopites from Suwalki. Because charges in the interlayer site are relatively constant (0.95–1.04), the deficit of positive charge due to the low Si/(Al + Fe) ratio (1.97–2.47) in tetrahedral site must be compensated by the incorporation of highly charged octahedral cations like Ti^{4+} or Al^{3+}.

As mentioned above and discussed by many authors (*e.g.* Kunitz, 1936; Edgar & Arima, 1983; Dymek, 1983; Abrecht & Hewitt, 1988; Brigatti *et al.*, 1991; Zhang *et al.*, 1993), a controversy is still present on the Ti occupancy in the phlogopite structure. If Ti is present in tetrahedral coordination, two substitution mechanism are theoretically possible: $^{[4]}Ti^{4+} = {}^{[4]}Si^{4+}$ and $({}^{[6]}Mg^{2+}, {}^{[6]}Fe^{2+}, {}^{[6]}Mn^{2+}) + 2{}^{[4]}Al^{3+} = {}^{[6]}\square + 2{}^{[4]}Ti^{4+}$. The majority of optical and Mössbauer spectral study, present in literature, have failed to conclude that titanium can occur in the tetrahedral site of natural phlogopites. In addition, the absence of significant correlation between Ti and $^{[4]}Si$ or $^{[4]}Al$ clearly indicate that these substitution mechanisms do not have played a role in the phlogopites from Suwalki. For this reason, Ti was only considered in octahedral coordination in this study.

Figure 1 shows that the Ti enrichment is mainly realized by the replacement of $({}^{[6]}Mg^{2+} + {}^{[6]}Fe^{2+} + {}^{[6]}Mn^{2+})$. Figure 4a represents the evolution of the Ti content as a function of $({}^{[6]}Mg^{2+} + {}^{[6]}Fe^{2+} + {}^{[6]}Mn^{2+})$. Two different patterns are observed.

The first trend concerns the more evolved (gabbronoritic) samples (K57-02 and Pig-05) characterized by a low Ti content. This trend shows a very good correlation (r^2 = 97 %) between the two terms of the diagram and a slope of *ca.* −1.96. This slope is very close to −2.0, corresponding to the theoretical slope for the reaction (Ti-vacancy substitution):

$$^{[6]}Ti^{4+} + {}^{[6]}\square = 2\left({}^{[6]}Mg^{2+}, {}^{[6]}Fe^{2+}, {}^{[6]}Mn^{2+}\right).$$

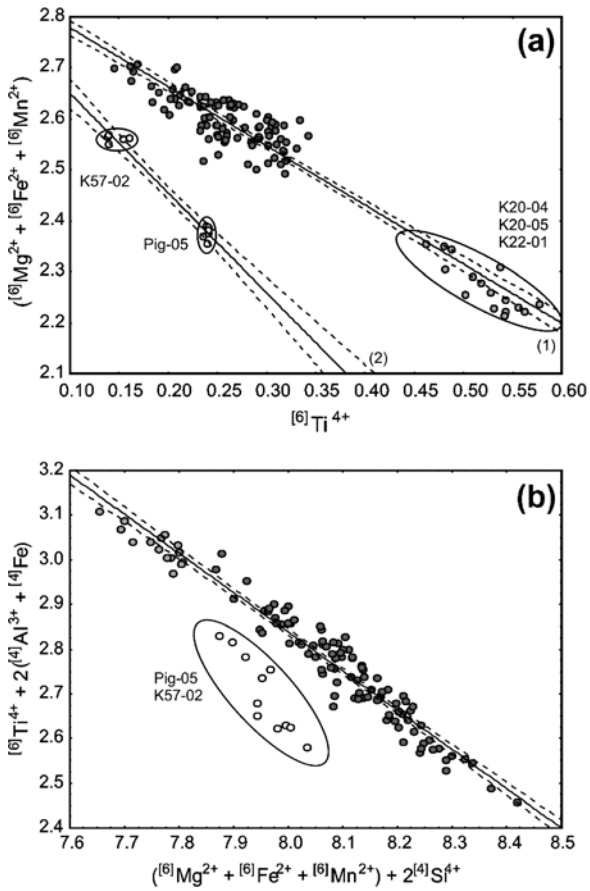

Fig. 4. Binary diagrams showing the relations between the different cations involved in the $^{[6]}Ti^{4+}$ substitution mechanisms. The dotted curves represent the 95 % confidence interval. (a): Binary diagram: $^{[6]}Ti^{4+} - (^{[6]}Mg^{2+} + {}^{[6]}Fe^{2+} + {}^{[6]}Mn^{2+})$. The curve labelled (1) is represented by the equation: $(^{[6]}Mg^{2+} + {}^{[6]}Fe^{2+} + {}^{[6]}Mn^{2+}) = 2.8949 - 1.159^{[6]}Ti^{4+}$ and has a correlation of about 92 %. The second trend labelled (2) is described by the equation: $(^{[6]}Mg^{2+} + {}^{[6]}Fe^{2+} + {}^{[6]}Mn^{2+}) = 2.8452 - 1.956^{[6]}Ti^{4+}$ and the correlation coefficient is 97 %. (b): Binary diagram $(^{[6]}Mg^{2+} + {}^{[6]}Fe^{2+} + {}^{[6]}Mn^{2+}) + 2^{[4]}Si^{4+} - {}^{[6]}Ti^{4+} + 2(^{[4]}Al^{3+} + {}^{[4]}Fe^{3+})$. The intermediate and high Ti content groups define a linear trend represented by the equation: $^{[6]}Ti^{4+} + 2(^{[4]}Al^{3+} + {}^{[4]}Fe^{3+}) = 11.064 - 1.078\,[(^{[6]}Mg^{2+} + {}^{[6]}Fe^{2+}) + 2^{[4]}Si^{4+}]$ showing a correlation of about 95 %.

The incorporation of one Ti is thus achieved by its replacement by two ($^{[6]}Mg^{2+}$, $^{[6]}Fe^{2+}$, $^{[6]}Mn^{2+}$) cations and is responsible for the introduction of one octahedral vacancy. Such a substitution model is consistent with experimental studies of Abrecht & Hewitt (1988) and with the results of the crystal chemical study realized by Brigatti *et al.* (1991) and by Matarrese *et al.* (2008) on phlogopites from different environments. However, this reaction enables the incorporation of a relatively limited Ti content.

The second trend concerns the two other groups of samples containing an intermediate and a high Ti content. The linear trend shows a good correlation (r^2 = 92 %) and a slope of *ca.* −1.2. This slope is relatively close to −1.0 and its interpretation is ambiguous. Indeed, along this line, the variation of one Ti a.p.f.u. is balanced by the replacement of one divalent cation ($^{[6]}Mg^{2+}$, $^{[6]}Fe^{2+}$, $^{[6]}Mn^{2+}$). This substitution can reflect two different mechanisms:

$$^{[6]}Ti^{4+} + 2^{[4]}Al^{3+} = \left(^{[6]}Mg^{2+} + {}^{[6]}Fe^{2+} + {}^{[6]}Mn^{2+}\right) + 2^{[4]}Si^{4+}$$

(Ti-Tschermak substitution)

or

$$Ti^{4+} + 2O^{2-} = \left(^{[6]}Mg^{2+} + {}^{[6]}Fe^{2+} + {}^{[6]}Mn^{2+}\right) + 2OH^{-}$$

(Deprotonation mechanism).

On Fig. 4b, data are plotted on a $^{[6]}Ti^{4+} + 2^{[4]}Al^{3+}$ *vs.* $(^{[6]}Mg^{2+} + {}^{[6]}Fe^{2+} + {}^{[6]}Mn^{2+}) + 2^{[4]}Si^{4+}$ diagram. The good correlation (r^2 = 95 %) is a clear evidence for the substitution $^{[6]}Ti^{4+} + 2^{[4]}Al^{3+} = (^{[6]}Mg^{2+} + {}^{[6]}Fe^{2+} + {}^{[6]}Mn^{2+}) + 2^{[4]}Si^{4+}$, as the linear trend has a slope (−1.08) practically identical to the theoretical slope (−1.0).

The deprotonation substitution

Recent studies have proposed that deprotonation (Dyar *et al.*, 1993) can be an important Ti substitution mechanism in natural phlogopites at high temperature, either in metamorphic or in magmatic rocks (Dyar *et al.*, 1993; Waters & Charnley 2002; Cesare *et al.*, 2003; Scordari *et al.*, 2006; Matarrese *et al.*, 2008). In this substitution model, OH^- is replaced by O^{2-} according to the equation:

$$\left(^{[6]}Mg^{2+} + {}^{[6]}Fe^{2+}\right) + 2OH^{-} = {}^{[6]}Ti^{4+} + 2O^{2-}$$

(Dyar *et al.*, 1993).

The possibility of a subordinate deprotonation mechanism associated with the Ti incorporation in the Ti-rich phlogopites at Suwalki cannot be assessed here, due to the lack of reliable water-content determination.

Fe^{3+} substitution mechanism

The Mössbauer spectral investigation of phlogopites from Suwalki showed that 0.046–0.167 a.p.f.u. Fe^{3+} occur on the octahedral sites of the structure. According to the literature (Matarrese *et al.*, 2008), the substitution mechanism responsible for the insertion of Fe^{3+} is:

$$3\left(^{[6]}Mg^{2+}, {}^{[6]}Fe^{2+}\right) = 2\left(^{[6]}Al^{3+}, {}^{[6]}Fe^{3+}\right) + {}^{[6]}\square\left(M^{3+}\text{-vacancy}\right)$$

According to Redhammer *et al.* (2000), the absorption band at *ca.* 3660 cm^{-1}, in the infrared spectra of synthetic micas on the annite-siderophyllite solid solution, is affected by the Fe^{3+} content. We attempted to correlate the Fe^{3+} content of the samples from Suwalki with the area of the band around 3660 cm^{-1}, but unfortunately the correlation was very poor.

Geothermometry

The amount of Ti incorporation in phlogopites was previously considered to essentially depend on temperature and

potential geothermometric applications were proposed (Engel & Engel, 1960; Robert 1976; Dymek 1983). However, as discussed above, it seems that the Ti enrichment in phlogopites depends on many parameters such as temperature, pressure and crystal chemistry (Guidotti, 1984; Henry & Guidotti, 2002).

Several studies realized on natural phlogopites from metamorphic rocks showed that the Ti content of these phlogopites increase with the metamorphic grade (Guidotti, 1984; Waters & Charnley, 2002). These observations were used by Henry & Guidotti (2002) and Henry *et al.* (2005) to calculate a Ti-saturation surface for natural phlogopites. This saturation surface is represented by a multi-dimensional surface depending on the Ti content, the Mg-content and the temperature. Equations are calibrated with a data set of phlogopites from metapelites from West Maine and South-Central Massachusetts. It can be written:

$\mathrm{Ln}\ z = a + bx^3 + cy^3$, where $a = -2.3594$, $b = 4.6482 \cdot 10^{-9}$, and $c = -1.7283$, and function of the temperature (x), the Mg# (Mg/(Mg + Fe); y), and the Ti content of phlogopite (z) (Henry *et al.*, 2005). Initially, this thermometer was developed only for a very narrow range of bulk compositions (metapelites with quartz, graphite, and a Ti-saturating mineral). However, it seems that this equation can be applied to a larger spectrum of bulk compositions if the mineral assemblage contains a Ti-saturating phase as ilmenite or rutile (Henry, pers. comm.).

Temperatures calculated for the phlogopites of Suwalki cumulates vary from 729 ± 15 to 874 ± 15 °C (Table 1). This range of temperature suggests that phlogopites from Suwalki have not experienced any metamorphic event responsible for a thermal reequilibration after crystallisation. In this case, a unique equilibrium temperature would be obtained with the Ti-in-phlogopite geothermometer. In addition, these temperatures are in perfect agreement with the experimental results obtained by Vander Auwera *et al.* (1998) and Bogaerts *et al.* (2006) on the basis of jotunitic liquids which are very close to the ferrodioritic magma of Suwalki. In fact, these authors have showed that all the liquidus phases (plagioclase, orthopyroxene, magnetite, ilmenite, and apatite) appear in a range of temperature between 1120 and 1050 °C. In the studied rocks, phlogopite corresponds to a late intercumulus mineral which must crystallize from the trapped liquid at lower temperatures than the liquidus phases.

Conclusions

Recently, several papers were published on the crystal-chemistry of titanian phlogopites with TiO_2 contents around 3.12–3.63 wt.% (Scordari *et al.*, 2006) or 2.34–6.02 wt.% (Matarrese *et al.*, 2008). The occurrence of phlogopites with very high TiO_2 contents reaching 9.41 wt.%, in the Suwalki anothosite (NE Poland), motivated the present crystal-chemical study.

Extensive electron-microprobe analyses of selected phlogopites, coupled with measurements by Mössbauer spectroscopy, infrared spectroscopy, and thermal analysis, indicated that the incorporation of $^{[6]}Ti^{4+}$ in the octahedral sites of the phlogopite structure is mainly assessed by vacancy formation (Ti-vacancy substitution) and complex exchanges between tetrahedral and octahedral cations (Ti-Tschermak substitution).

Acknowledgements: Many thanks are due to E. Rampone, P. Comodi, and an anonymous reviewer for their constructive comments. This study was funded by the Belgian Fund for Joint Research. Fieldwork was financed by the CGRI (Commission Générale pour les Relations Internationales de la Communauté française de Belgique) and by a Student Research Grant from the Society for Economic Geologists. We acknowledge J. Wiszniewska from the Polish Geological Institute for giving access to drill-cores and C.E. Morisset for help in collecting samples. Microprobe analyses were done under the supervision of H.J. Bernhardt (University of Bochum, Germany). O.N., F.H., F.G., and A.-M.F. acknowledge the "Fonds National de la Recherche Scientifique" (Belgium) for a Ph. D. grant (FRIA), for a position of "Chercheur qualifié", and for grants 1.5.112.02, 9.456595, and 1.5.064.05.

References

Abrecht, J. & Hewitt, D.A. (1988): Experimental evidence on the substitution of Ti in biotite. *Am. Mineral.*, **73**, 1275-1284.

Arima, M. & Edgar, A.D. (1981): Substitution mechanisms and solubility of titanium in phlogopites from rocks of probable mantle origin. *Contrib. Mineral. Petrol.*, **77**, 288-295.

Badreddine, R., Grandjean, F., Vandormael, D., Fransolet, A.-M., Long, G.J. (2000): An iron-57 Mössbauer spectral study of vermiculitization in the Palabora complex, Republic of South Africa. *Clay Minerals*, **35**, 653-663.

Bogaerts, M., Scaillet, B., Vander Auwera, J. (2006): Phase equilibria of the Lyngdal granodiorite (Norway): implications for the origin of metaluminous ferroan granitoids. *J. Petrol.*, **47**, 2405-2431.

Brigatti, M.F., Galli, E., Poppi, L. (1991): Effect of Ti substitution in biotite-1M crystal chemistry. *Am. Mineral.*, **76**, 1174-1183.

Cesare, B., Cruciani, G., Russo, U. (2003): Hydrogen deficiency in Ti-rich biotite from anatectic metapelites (El Joyazo, SE Spain): crystal chemical aspects and implications for high-temperature petrogenesis. *Am. Mineral.*, **88**, 583-595.

Cesare, B., Satish-Kumar, M., Cruciani, G., Pocker, S., Nodari, L. (2008): Mineral chemistry of Ti-rich biotite from pegmatite and metapelitic granulites of the Kerala Khondalite Belt (southeast India): petrology and further insight into titanium substitutions. *Am. Mineral.*, **93**, 327-338.

Coey, J.M.D. (1984): Mössbauer spectroscopy of silicate minerals. *in* "Mössbauer Spectroscopy Applied to Inorganic Chemistry", vol. 1, G.J. Long, ed. Plenum Press, New-York, USA. 443-510.

Cruciani, G. & Zanazzi, P.F. (1994): Cation partitioning and substitution mechanisms in 1*M* phlogopite: a crystal chemical study. *Am. Mineral.*, **79**, 289-301.

Dörr, W., Belka, Z., Marheine, D., Schastok, J., Valverde-Vaquero, P., Wiszniewska, J. (2002): U–Pb and Ar–Ar geochronology of anorogenic granite magmatism of the Mazury complex, NE Poland. *Prec. Res.*, **119**, 101-120.

Dyar, M.D. (1987): A review of Mössbauer data on trioctahedral micas: evidence for tetrahedral Fe^{3+} and cation ordering. *Am. Mineral.*, **72**, 102-112.

Dyar, M.D., Guidotti, C.V., Holdaway, M.J., Colucci, M. (1993): Nonstoichiometric hydrogen contents in common rock-forming hydroxyl silicates. *Geochim. Cosmochim. Acta*, **57**, 2913-2918.

Dymek, R.F. (1983): Titanium, aluminium and interlayer cation substitutions in biotite from high-grade gneisses, West Greenland. *Am. Mineral.*, **68**, 880-889.

Edgar, A.D. & Arima, M. (1983): Conditions of phlogopite crystallization in ultrapotassic volcanic rocks. *Mineral. Mag.*, **47**, 11-19.

Edgar, A.D., Green, D.H., Hibberson, W.O. (1976): Experimental petrology of a highly potassic magma. *J. Petrol.*, **17**, 339-356.

Engel, A.E.J. & Engel, C.G. (1960): Progressive metamorphism and granitization of the major paragneiss, northwest Adirondack Mountains, New York, Part 2. Mineralogy. *Bull. Geol. Soc. Am.*, **71**, 1-58.

Farmer, V.C. (1971): Evidence for loss of protons and octahedral iron from oxidized biotites and vermiculites. *Mineral. Mag.*, **38**, 121-137.

Feldstein, S.N., Lange, R.A., Vennemann, T., O'Neil, J.R. (1996): Ferric–ferrous ratios, H_2O contents and D/H ratios of phlogopite and biotite from lavas of different tectonic regimes. *Contrib. Mineral. Petrol.*, **126**, 51-66.

Forbes, W.C. & Flower, M.F.J. (1974): Phases relations of titan-phlogopite, $K_2Mg_4TiAl_2Si_6O_{20}(OH)_4$: a refractory phase in the upper mantle? *Earth Planet. Sci. Lett.*, **22**, 60-66.

Guidotti, C.V. (1984): Micas in metamorphic rocks. *in* "Micas", S.W. Bailey, ed. *Rev. Mineral.*, **13**, Mineralogical Society of America, Washington, DC, 357-468.

Guidotti, C.V., Cheney, J.T., Guggenheim, S. (1977): Distribution of titanium between coexisting muscovite and biotite in pelitic schists from northwestern Maine. *Am. Mineral.*, **62**, 438-448.

Henry, D.J. & Guidotti, C.V. (2002): Titanium in biotite from metapelitic rocks: temperature effects, crystal-chemical controls, and petrologic applications. *Am. Mineral.*, **87**, 375-382.

Henry, D.J., Guidotti, C.V., Thomson, J.A. (2005): The Ti-saturation surface for low-to-medium pressure metapelitic biotites: implications for geothermometry and Ti-substitution mechanisms. *Am. Mineral.*, **90**, 316-328.

Ibhi, A., Nachit, H., El Abia, H. (2005): Titanium and barium incorporation into the phyllosilicate phases: the example of phlogopite–kinoshitalite solid solution. *J. Phys. IV-proceedings*, **123**, 331-335.

Kunitz, W. (1936): Beitrag zur Kenntnis der magmatischen Assoziationen III. Die Rolle des Titans und Zirkoniums in den gesteinsbildenden Silikaten. *N. Jb. Geol. Paläont.*, **70**, 385-416.

Ludington, D.S. & Munoz, J.L. (1975): Application of fluor-hydroxyl exchange data to natural micas. *Geol. Soc.* Am., Abstracts with Programs, **7**, 1179.

Matarrese, S., Schingaro, E., Scordari, F., Stoppa, F., Rosatelli, G., Pedrazzi, G., Ottolini, L. (2008): Crystal chemistry of phlogopite from Vulture-S. Michele Subsynthem volcanic rocks (Mt. Vulture, Italy) and volcanological implications. *Am. Mineral.*, **93**, 426-437.

Mitchell, R.H. (1985): A review of the mineralogy of lamproites. *Trans. Geol. Soc. S. Afr.*, **88**, 411-437.

Mitchell, R.H. & Bergman, S.C. (1991): Petrology of lamproites, Plenum, New York, 440 p.

Morgan, J.W., Stein, H.J., Hannah, J.L., Markey, R.J., Wiszniewska, J. (2000): Re–Os study of Fe–Ti–V oxide and Fe–Cu–Ni sulphide deposits, Suwalki Anorthosite Massif, Northeast Poland. *Mineral. Deposita*, **35**, 391-401.

Oxford Diffraction. (2002): CrysAlis CCD and CrysAlis RED Version 1.69. Oxford Diffraction, Oxford, England.

Papin, A., Sergent, J., Robert, J.L. (1997): Intersite OH–F distribution in an Al-rich phlogopite. *Eur. J. Mineral.*, **9**, 501-508.

Patiño Douce, A.E., Johnston, A.D., Rice, J.M. (1993): Erratum. Octahedral excess mixing properties in biotite: a working model with applications to geobarometry and geothermometry. *Am. Mineral.*, **78**, 826.

Petit, S., Robert, J.L., Decarreau, A., Besson, G., Grauby, O., Martin, F. (1995): Contribution of spectroscopic methods to 2:1 clay caracterization. *Bulletin des Centres de Recherches Exploration-Production Elf Aquitaine*, **19**, 119-147.

Rancourt, D.G., Mercier, P.H.J., Cherniak, D.J., Desgreniers, S., Kodama, H., Robert, J.L., Murad, E. (2001): Mechanisms and crystal chemistry of oxidation in annite: resolving the hydrogen-loss and vacancy reactions. *Clays Clay Mineral.*, **6**, 455-491.

Redhammer, G.J., Beran, A., Schneider, J., Amthauer, G., Lottermoser, W. (2000): Spectroscopic and structural properties of synthetic micas on the annite-siderophyllite binary: synthesis, crystal structure refinement, Mössbauer, and infrared spectroscopy. *Am. Mineral.*, **85**, 449-465.

Rieder, M., Cavazzini, G., D'Yakonov, Y., Frank-Kamenetskii, V.A., Gottardi, G., Guggenheim, S., Koval, P.V., Müller, G., Neiva, A.M.R., Radoslovich, E.W., Robert, J.L., Sassi, F.P., Takeda, H., Weiss, Z., Wones, D.R. (1998): Nomenclature of the micas. *Can. Mineral.*, **36**, 41-48.

Righter, K., Dyar, M.D., Delaney, J.S., Vennemann, T.W., Hervig, R.L., King, P.L. (2002): Correlations of octahedral cations with OH^-, O^{2-}, Cl^- and F^- in biotite from volcanic rocks and xenoliths. *Am. Mineral.*, **87**, 142-153.

Robert, J.L. (1976): Titanium solubility in synthetic phlogopite solid solutions. *Chem. Geol.*, **17**, 213-227.

Robert, J.L., Beny, J.M., Della Ventura, G., Hardy, M. (1993): Fluorine in micas: crystal-chemical control of the OH–F distribution between trioctahedral and dioctahedral sites. *Eur. J. Mineral.*, **5**, 7-18.

Robert, J.L., Hardy, M., Sanz, J. (1995): Excess protons in synthetic micas with tetrahedrally coordinated divalent cations. *Eur. J. Mineral.*, **7**, 457-461.

Scordari, F., Venturi, G., Sabato, A., Bellatreccia, F., Della Ventura, G., Pedrozzi, G. (2006): Ti-rich phlogopite from Mt. Vulture (Potenza, Italy) investigated by a multianalytical approach: substitutional mechanisms and orientation of the OH dipoles. *Eur. J. Mineral.*, **18**, 379-391.

Tronnes, R.G., Edgar, A.D., Arima, M. (1985): A high pressure-high temperature study of TiO_2 solubility in Mg-rich phlogopite: implications to phlogopite chemistry. *Geochim. Cosmochim. Acta*, **49**, 2323-2329.

Vander Auwera, J., Longhi, J., Duchesne, J.C. (1998): A liquid line of descent of the jotunite (hypersthene monzodiorite) suite. *J. Petrol.*, **39**, 439-468.

Vedder, W. & Wilkins, R.W.T. (1969): Dehydroxylation and rehydroxylation, oxidation and reduction of micas. *Am. Mineral.*, **54**, 483-509.

Virgo, D. & Popp, R.K. (2000): Hydrogen deficiency in mantle-derived phlogopites. *Am. Mineral.*, **85**, 753-759.

Wagner, C. & Velde, D. (1986): The mineralogy of K-richterite-bearing lamproites. *Am. Mineral.*, **71**, 17-37.

Waters, D.J. & Charnley, N.R. (2002): Local equilibrium in polymetamorphic gneiss and the titanium substitution in biotite. *Am. Mineral.*, **87**, 383-396.

Wilkins, R.W.T. (1967): The hydroxyl-stretching region of the biotite mica spectrum. *Mineral. Mag.*, **36**, 325-333.

Zhang, M., Suddaby, P., Thompson, R.N., Dungan, M.A. (1993): Barian–titanian phlogopite from potassic lavas in northeast China: chemistry, substitutions and paragenesis. *Am. Mineral.*, **78**, 1056-1065.

Received 16 May 2008
Modified version received 29 July 2008
Accepted 4 September 2008